



Contents lists available at ScienceDirect

International Communications in Heat and Mass Transfer

journal homepage: www.elsevier.com/locate/ichmt

Double-diffusive turbulent natural convection in a porous square cavity with opposing temperature and concentration gradients[☆]

Luzia A. Tofaneli, Marcelo J.S. de Lemos^{*}

Departamento de Energia–IEME, Instituto Tecnológico de Aeronáutica–ITA, 12228-900–São José dos Campos–SP, Brazil

ARTICLE INFO

Available online 23 July 2009

Keywords:

Porous media
Double-diffusion
Turbulence modeling
Natural convection

ABSTRACT

This paper presents results for coupled heat and mass transport under laminar and turbulent flow regimes in porous cavities. Two driving mechanisms are considered to contribute to the overall momentum transport, namely temperature driven and concentration driven mass fluxes. Aiding and opposing flows are considered, where temperature and concentration gradients are either in the same direction or of different sign, respectively. Modeled equations are presented based on the double-decomposition concept, which considers both time fluctuations and spatial deviations about mean values. Turbulent transport is accounted for via a macroscopic version of the k - ϵ model. Variation of the cavity Nusselt and Sherwood numbers due to changes on N , where N is the ratio of solute to thermal Grashof numbers, is presented. Results indicate that for aiding cases, mass and heat transfer across the cavity are enhanced faster than for cases with opposing temperature and concentration gradients. For the conditions here investigated, the use a turbulence model gave results for Nu and Sh that were nearly double when compared with laminar results for the same conditions.

© 2009 Elsevier Ltd. All rights reserved.

1. Introduction

The study of double-diffusive natural convection in porous media has many environmental and industrial applications, including grain storage and drying, petrochemical processes, oil and gas extraction, contaminant dispersion in underground water reservoirs and electrochemical processes, to mention a few. The importance of double-diffusive natural convection can be better appreciated by the volume of papers published in this field, which was reviewed recently by Nield and Bejan [1].

Accordingly, double-diffusive convection in a vertical cavity subject to horizontal temperature gradients has been investigated by Trevisan and Bejan [2,3], Goyeau et al. [4], Mamou et al. [5,6], Mohamad and Bennacer [7], Nithiarasu et al [8] and Bennacer et al [9,10], among others. In most of the aforementioned papers, the intrapore flow was assumed to be laminar and it was demonstrated that, depending on the governing parameters of the problem and on the thermal to solute buoyancy ratio, various modes of convection prevail. However, in some specific applications, the fluid mixture may become turbulent and difficulties arise in the proper mathematical modeling of the transport processes under both temperature and concentration gradients. Due to such difficulties, there seems to be a lack in the literature on turbulent solution of double-diffusive convection.

Motivated by the foregoing, in an earlier paper [11] a mathematical framework for treating turbulent double-diffusive flows in porous media was presented, but no numerical simulations were published.

That work was derived from a general mathematical model for turbulent flow in porous media [12], which was developed under a concept called “double-decomposition” [13]. Such concept considered time fluctuations of the flow properties in addition to spatial deviations, in relation to a volume-average, when setting up macroscopic equations for the flow. Using such concept, non-buoyant [14] as well as buoyant heat transfer has been considered [15–18] in addition to turbulent mass transfer [19]. Application of such methodology to channel flows with porous inserts [20,21] have also been presented. However, in none of the above applications, results for turbulent double-diffusion in porous media were presented.

The purpose of this contribution is to show numerical results for turbulent double-diffusive in porous media, which are obtained with the mathematical model earlier proposed in [11]. To the best of the authors’ knowledge, no solutions for turbulent flow using the work in [11] have been previously published. Here, both aiding and opposing cases are investigated.

2. Macroscopic mathematical model

The problem considered here is showed schematically in Fig. 1a and refers to a square cavity containing a saturated porous medium. The cavity of height H , width L and aspect ratio $A = H/L = 1$ is filled with a binary fluid. The enclosure is isothermally heated from the left and cooled from the opposing side. The top and bottom walls are kept insulated and the porous medium is considered to be rigid. The binary fluid in the cavity of Fig. 1a is assumed to be Newtonian and to satisfy the Boussinesq approximation.

[☆] Communicated by W.J. Minkowycz.

^{*} Corresponding author.

E-mail address: delemos@ita.br (M.J.S. de Lemos).

Nomenclature

A	aspect ratio
c_F	Forchheimer coefficient
c_p	specific heat
C	mass concentration
Da	Darcy number, $Da = K/H^2$
\mathbf{D}_{disp}	mass dispersion tensor
$\mathbf{D}_{disp,t}$	turbulent mass dispersion tensor
D	mass transfer coefficient
\mathbf{D}_t	turbulent mass flux tensor
\mathbf{g}	gravity acceleration vector
G_β^i	Generation rate of $\langle k \rangle^i$ due to buoyant effects
$Gr_{c\phi}$	solute Grashof number based on H , $Gr_{c\phi} = g\beta_{c\phi}\Delta CH^3/v^2$
Gr_ϕ	thermal Grashof number based on H , $Gr_\phi = g\beta_\phi\Delta TH^3/v^2$
H	height of enclosure
k	turbulent kinetic energy per unit mass, $k = \overline{\mathbf{u}' \cdot \mathbf{u}'}/2$
$\langle k \rangle^i$	intrinsic (fluid) average of k
K	permeability
\mathbf{K}_{disp}	Conductivity tensor due to dispersion
$\mathbf{K}_{disp,t}$	Conductivity tensor due to turbulent dispersion
\mathbf{K}_t	Conductivity tensor due to turbulent heat flux
\mathbf{K}_{tor}	Conductivity tensor due to tortuosity
Le	Lewis number, $Le = Sc/Pr = D/\alpha$
N	buoyancy ratio, $N = Gr_{c\phi}/Gr_\phi$, $N = 0$ for thermal drive only.
Nu	Nusselt number
p	pressure
Pr	Prandtl number, $Pr = \nu/\alpha$
Ra^*	Rayleigh–Darcy number, $Ra^* = Gr_\phi Pr Da (\alpha/\alpha_{eff})$, $\alpha_{eff} = \lambda_{eff}/(\rho c_p)_f$
Sc	Schmidt number, $Sc = \nu/D$
Sh	Sherwood number
T	temperature
\mathbf{u}	velocity of the mixture
$\bar{\mathbf{u}}_D$	Darcy velocity vector

Greek symbols

α	fluid thermal diffusivity, $\alpha = \lambda_f/(\rho c_p)_f$
β_ϕ	macroscopic thermal expansion coefficient
$\beta_{c\phi}$	macroscopic solute expansion coefficient
ΔC	concentration difference between plates, $C_1 - C_2$
ΔT	concentration difference between plates, $T_1 - T_2$
$\lambda_{(s,f)}$	fluid/solid thermal conductivity
λ_{eff}	effective thermal conductivity, $\lambda_{eff} = (1 - \phi)\lambda_f + \phi\lambda_s$
μ	fluid mixture viscosity
$\mu_{t\phi}$	macroscopic turbulent viscosity
ε	dissipation rate of k
$\langle \varepsilon \rangle^i$	intrinsic (fluid) average of ε
ρ	bulk density of the mixture
ϕ	porosity

Subscripts

β	buoyancy
\prime	chemical species
t	turbulent
ϕ	macroscopic
C	concentration
T	temperature
(s, f)	solid/fluid

Superscripts

i	intrinsic (fluid) average
v	volume (fluid + solid) average

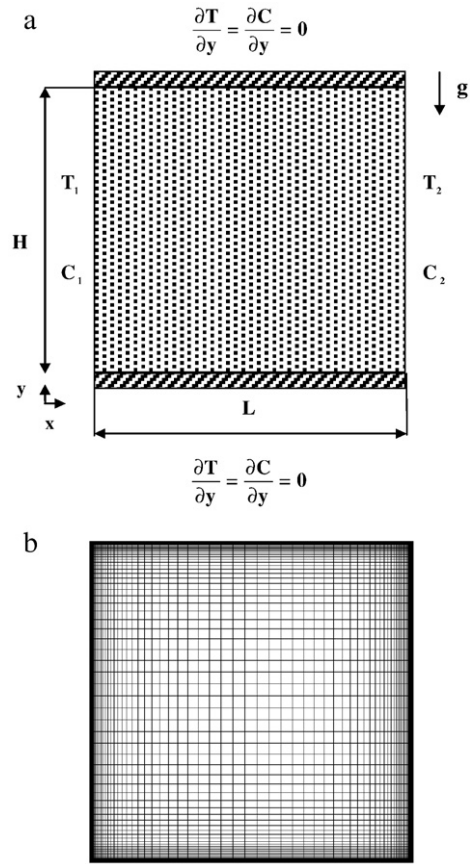


Fig. 1. Configuration investigated: a) geometry and boundary conditions, b) stretched grid.

The equations used herein are derived in details in [11–13] and for that their derivation need not be repeated here. They are developed based on volume-averaging procedures which are fully described in the literature [22–25].

The macroscopic continuity equation is then given by,

$$\nabla \bar{\mathbf{u}}_D = 0 \quad (1)$$

where the Dupuit–Forchheimer relationship, $\bar{\mathbf{u}}_D = \phi \langle \bar{\mathbf{u}} \rangle^i$, has been used and $\langle \bar{\mathbf{u}} \rangle^i$ identifies the intrinsic (liquid) average of the local velocity vector $\bar{\mathbf{u}}$. The macroscopic time-mean Reynolds equation for an incompressible fluid with constant properties is given as,

$$\begin{aligned} \rho \nabla \cdot \left(\frac{\bar{\mathbf{u}}_D \bar{\mathbf{u}}_D}{\phi} \right) = & -\nabla \cdot (\phi \langle \bar{p} \rangle^i) + \mu \nabla^2 \bar{\mathbf{u}}_D + \nabla \cdot (-\rho \phi \langle \bar{\mathbf{u}}' \bar{\mathbf{u}}' \rangle^i) \\ & - \rho g \phi [\beta_\phi (\langle \bar{T} \rangle^i - T_{ref}) + \beta_{c\phi} (\langle \bar{C} \rangle^i - C_{ref})] \\ & - \left[\frac{\mu \phi}{K} \bar{\mathbf{u}}_D + \frac{c_F \phi \rho}{\sqrt{K}} |\bar{\mathbf{u}}_D| \bar{\mathbf{u}}_D \right] \end{aligned} \quad (2)$$

where the last two terms in Eq. (2) represent the Darcy–Forchheimer contribution. The symbol K is the porous medium permeability, c_F is the form drag coefficient (Forchheimer coefficient), $\langle \bar{p} \rangle^i$ is the intrinsic average pressure of the fluid, ρ is the fluid density, μ represents the fluid viscosity and ϕ is the porosity of the porous medium. Buoyancy effects due to temperature and concentration variations within the cavity are also shown in Eq. (2). The macroscopic Reynolds stress $-\rho \phi \langle \bar{\mathbf{u}}' \bar{\mathbf{u}}' \rangle^i$ is modeled as,

$$-\rho \phi \langle \bar{\mathbf{u}}' \bar{\mathbf{u}}' \rangle^i = \mu_t \langle \bar{\mathbf{D}} \rangle^v - \frac{2}{3} \phi \rho \langle k \rangle^i \mathbf{I} \quad (3)$$

where

$$\langle \mathbf{D} \rangle^v = \frac{1}{2} \left[\nabla(\phi \langle \bar{\mathbf{u}} \rangle^i) + [\nabla(\phi \langle \bar{\mathbf{u}} \rangle^i)]^T \right] \quad (4)$$

is the macroscopic deformation tensor, $\langle k \rangle^i = \overline{\langle \mathbf{u}' \cdot \mathbf{u}' \rangle}^i / 2$ is the intrinsic turbulent kinetic energy and $\mu_{t\phi}$ is the turbulent viscosity, which is modeled in [13] similarly to the case of clear flow, in the form,

$$\mu_{t\phi} = \rho c_\mu \frac{\langle k \rangle^i}{\langle \varepsilon \rangle^i} \quad (5)$$

Coefficients β_ϕ and $\beta_{c\phi}$ in Eq. (2) are used to write the Grashof numbers associated with the thermal and solute drives, in the form,

$$Gr_\phi = \frac{g\beta_\phi \Delta T H^3}{\nu^2}, Gr_{c_\phi} = \frac{g\beta_{c_\phi} \Delta C H^3}{\nu^2} \quad (6)$$

where $\Delta T = T_1 - T_2$ and $\Delta C = C_1 - C_2$ are the maximum temperature and concentration variation across the cavity, respectively. One should note that for opposing thermal and concentrations drives, such maximum differences are of opposing sign. Also, the Rayleigh–Darcy number is a dimensionless parameter defined as $Ra^* = g\beta_\phi \Delta T H K / \nu \alpha_{\text{eff}}$, with $\alpha_{\text{eff}} = \lambda_{\text{eff}} / (\rho c_p)_f$.

The ratio of Grashof numbers defines the buoyancy ratio, N , in the form

$$N = \frac{Gr_{c_\phi}}{Gr_\phi} = \frac{\beta_{c_\phi} \Delta C}{\beta_\phi \Delta T} \quad (7)$$

giving for Eq. (2),

$$\begin{aligned} \rho \nabla \cdot \left(\frac{\bar{\mathbf{u}}_D \bar{\mathbf{u}}_D}{\phi} \right) &= -\nabla(\phi \langle \bar{p} \rangle^i) + \mu \nabla^2 \bar{\mathbf{u}}_D + \nabla \cdot (-\rho \phi \langle \overline{\mathbf{u}' \mathbf{u}'} \rangle^i) \\ &\quad - \rho g \phi \beta_\phi \left\{ \langle \bar{T} \rangle^i - \bar{T}_{\text{ref}} + N \frac{\Delta T}{\Delta C} (\langle \bar{C} \rangle^i - \bar{C}_{\text{ref}}) \right\} \\ &\quad - \left[\frac{\mu \phi}{K} \bar{\mathbf{u}}_D + \frac{c_F \phi \rho}{\sqrt{K}} |\bar{\mathbf{u}}_D| \right] \end{aligned} \quad (8)$$

Either $\beta_{c\phi} = 0$ or $\Delta C = 0$ results in $N = 0$, or say, only thermal drive applies. Also, for $\beta_{c\phi} = 0$ and $\Delta C \neq 0$ in Eq. (8), although no concentration drive is modeled, a distribution of C within the field will occur due to the flow established by the thermal drive.

Additional transport equations read (see [11] for details).

2.1. Heat transport

$$(\rho c_p)_f \nabla \cdot (\bar{\mathbf{u}}_D \langle \bar{T} \rangle^i) = \nabla \cdot \{ \mathbf{K}_{\text{eff}} \cdot \nabla \langle \bar{T} \rangle^i \} \quad (9)$$

$$\mathbf{K}_{\text{eff}} = \underbrace{[\phi \lambda_f + (1-\phi) \lambda_s]}_{\lambda_{\text{eff}}} \mathbf{I} + \mathbf{K}_{\text{tor}} + \mathbf{K}_t + \mathbf{K}_{\text{disp}} + \mathbf{K}_{\text{disp},t} \quad (10)$$

2.2. Mass transport

$$\nabla \cdot (\bar{\mathbf{u}}_D \langle \bar{C} \rangle^i) = \nabla \cdot \mathbf{D}_{\text{eff}} \cdot \nabla(\phi \langle \bar{C} \rangle^i) \quad (11)$$

$$\mathbf{D}_{\text{eff}} = \mathbf{D}_{\text{disp}} + \mathbf{D}_{\text{diff}} + \mathbf{D}_t + \mathbf{D}_{\text{disp},t} \quad (12)$$

$$\mathbf{D}_{\text{diff}} = \langle D \rangle^i \mathbf{I} = \frac{1}{\rho} \frac{\mu_b}{Sc} \mathbf{I} \quad (13)$$

$$\mathbf{D}_t + \mathbf{D}_{\text{disp},t} = \frac{1}{\rho} \frac{\mu_{t\phi}}{Sc_t} \mathbf{I} \quad (14)$$

Transport equations for $\langle k \rangle^i$ and its dissipation rate $\langle \varepsilon \rangle^i = \mu \langle \nabla \mathbf{u}' : (\nabla \mathbf{u}')^T \rangle^i / \rho$ including additional effects due to temperature and concentration gradients are proposed as in [11]:

$$\rho \nabla \cdot (\bar{\mathbf{u}}_D \langle k \rangle^i) = \nabla \cdot \left[\left(\mu + \frac{\mu_b}{Sc_k} \right) \nabla(\phi \langle k \rangle^i) \right] + P^i + G^i + G_\beta^i + G_{\beta_c}^i - \rho \phi \langle \varepsilon \rangle^i \quad (15)$$

$$\begin{aligned} \rho \nabla \cdot (\bar{\mathbf{u}}_D \langle \varepsilon \rangle^i) &= \nabla \cdot \left[\left(\mu + \frac{\mu_b}{Sc_\varepsilon} \right) \nabla(\phi \langle \varepsilon \rangle^i) \right] \\ &\quad + \frac{\langle \varepsilon \rangle^i}{\langle k \rangle^i} [c_1 P^i + c_2 G^i + c_3 (G_\beta^i + G_{\beta_c}^i) - c_2 \rho \phi \langle \varepsilon \rangle^i] \end{aligned} \quad (16)$$

where c_1, c_2, c_3 and c_k are constants. The generation rate of k due to buoyancy is represented by G_β^i and $G_{\beta_c}^i$ for both the thermal and solute drives, respectively [11].

3. Integral parameters

The local Nusselt number on the hot wall of the square cavity ($x = 0$) is defined as,

$$Nu_y = hL / \lambda_{\text{eff}} \therefore Nu_y = \left(\frac{\partial \langle T \rangle^i}{\partial x} \right)_{x=0} \frac{L}{T_1 - T_2} \quad (17)$$

where T_1 and T_2 refers to the temperature limits imposed at the cavity lateral walls (Fig. 1). The average Nusselt number is then given by,

$$Nu = \frac{1}{H} \int_0^H Nu_y dy \quad (18)$$

Likewise, the local Sherwood number on the wall where the highest concentration prevails, or say, at $x = 0$ for adding drives and at $x = L$ for opposing cases, can be defined as,

$$Sh_y = h_c L / D \therefore Sh_y = \left(\frac{\partial \langle C \rangle^i}{\partial x} \right)_{x_{\text{wall}}} \frac{L}{C_1 - C_2} \quad (19)$$

Here also 1 and 2 are subscripts referring to the maximum and minimum concentration values, respectively, and h_c is a film coefficient for mass transfer. The average Sherwood number is then given by,

$$Sh = \frac{1}{H} \int_0^H Sh_y dy \quad (20)$$

The variables h and h_c are local film coefficients for heat and mass transfer, respectively.

4. Numerical details

The numerical method employed for discretizing the governing equations is the control-volume approach. A hybrid scheme, which includes both the Upwind Differencing Scheme (UDS) and the Central Differencing Scheme (CDS), was used for interpolating the convection

Table 1

Average Nusselt and Sherwood numbers for thermal drive only, $N = 0$ with $\beta_{c\phi} = 0$, ($Le = 10, A = 1$).

Ra^*	Imposed conditions		100	200	400	1000	2000
Nu	$\frac{\Delta C}{\Delta T} = 1,$ $\beta_{c_\phi} = 0$	Present results	3.11	4.90	7.65	13.22	19.54
		Goyeau et al. [4]	3.11	4.96	7.77	13.47	19.90
		Trevisan and Bejan [2]	3.27	5.61	9.69	–	–
Sh		Present results	14.76	22.02	32.55	53.37	76.58
		Goyeau et al. [4]	13.25	19.86	28.41	48.32	69.29
		Trevisan and Bejan [2]	15.61	23.23	30.76	–	–

fluxes. The well-established SIMPLE algorithm [26] was followed for handling the pressure–velocity coupling. Individual algebraic equations sets were solved by the SIP procedure of [27]. In addition, concentration of nodal points closer to the walls reduces eventual errors due to numerical diffusion which, in turn, are further annihilated due to the hybrid scheme here adopted. Calculations for laminar and turbulent flows used a 80×80 stretched grid for all cases (Fig. 1b). For turbulent flow calculations, wall log laws were applied.

5. Results and discussion

As mentioned, this work refers to the study of natural convective flows in a porous cavity of height H , width L and aspect ratio $A = H/L = 1$ saturated by a binary fluid. The flow is incompressible and a two-dimensional steady state was assumed. Horizontal temperature and concentration differences were specified between the vertical walls (Fig. 1a).

The validation of the numerical code has been performed over a large range of parameters for purely thermal natural convection in porous media. Table 1 shows average Nusselt and Sherwood numbers for laminar flow compared with those by [2] and [4]. Results in the table consider mass transfer caused by thermal convection only ($N = 0$). In this configuration, the solute buoyancy force is not present but mass transfer across the cavity occurs due to the thermally driven flow. The table shows good agreement with similar computations presented in the literature and indicates correct programming of the numerical code developed.

Simulations considering laminar and turbulent flow for $\phi = 0.8$, $Ra^* = 2 \times 10^6$, $Pr = 10$, $Gr_\phi = 2.25 \times 10^{10}$, $Da = 8.88 \times 10^{-6}$, $\lambda_{eff} = \lambda_s = \lambda_f$ and $Le = 1.0$ are shown next. The buoyancy ratio N was varied from -5 to 5 , for both model solutions.

Fig. 2 shows the average Nusselt and Sherwood numbers at the heated wall as a function of N . For aiding flows ($N > 0$), Nu and Sh

increase with N . The figure also shows that there are significant variations between the laminar and turbulent model solutions, with integral values nearly doubling when turbulence is considered, at least for the particular conditions presented in the figure.

The case for $N = 0$ indicates that convection is sole due to thermal buoyancy. However, since the C-equation is also solved, the flow mixes the concentration field and a corresponding Sherwood is computed. The value of Nu is at minimum when $N = -1$, when the two driving mechanisms oppose each other with equal strength. Under such circumstances, conduction prevails across the cavity.

The figure further indicates that as N is decreased below -1 , negative buoyancy forces due to species distribution acts vertically downward, along the heated wall, thereby opposing the vertically upward thermal buoyancy drive. For that, transport rates are lower for $N < -1$ when compared with aiding cases having the same numerical value of $|N|$. That is, laminar Nu and Sh for $N = +4$ are 15% higher than for $N = -4$, for example. For turbulent solution, such differences for the same values of N are around 23% for both Nu and Sh .

6. Conclusions

This work presents numerical computations for laminar and turbulent flows using a macroscopic $k-\epsilon$ model with wall functions. Double-diffusive natural convection in a square cavity, totally filled with porous material, was simulated. The cavity was heated from the left and cooled from the opposing side. For aiding laminar flows, predicted integral parameters were 15% higher when compared with flows with similar but opposing conditions. For adding turbulent flows, Nu and Sh values are roughly 23% higher than for the cases of opposing flows, at least for the conditions here simulated.

Acknowledgments

The authors would like to thank the CNPq and the FAPESP, Brazil, for their invaluable financial support during the preparation of this work.

References

- [1] D.A. Nield, A. Bejan, Convection in porous media, Springer, Berlin, 1999.
- [2] O.V. Trevisan, A. Bejan, Natural convection with combined heat mass transfer buoyancy effects in a porous medium, International Journal Heat and Mass Transfer 28 (1985) 1597–1611.
- [3] O.V. Trevisan, A. Bejan, Mass and heat transfer by natural convection in a vertical slot filled with porous medium, International Journal Heat and Mass Transfer 29 (1986) 403–415.
- [4] B. Goyeau, J.P. Songbe, D. Gobin, Numerical study of double-diffusive natural convection in a porous cavity using the Darcy–Brinkman formulation, International Journal of Heat and Mass Transfer 39 (7) (1996) 1363–1378.
- [5] M. Mamou, P. Vasseur, E. Bilgen, Multiple solutions for double-diffusive convection in a vertical porous enclosure, International Journal of Heat and Mass Transfer 38 (10) (1995) 1787–1798.
- [6] M. Mamou, M. Hasnaoui, A. Amahmid, P. Vasseur, Stability analysis of double diffusive convection in a vertical Brinkman porous enclosure, International Communications in Heat and Mass Transfer 25 (4) (1998) 491–500.
- [7] A.A. Mohamad, R. Bennacer, Double diffusion natural convection in an enclosure filled with saturated porous medium subjected to cross gradients: stably stratified fluid, International Journal of Heat and Mass Transfer 45 (18) (2002) 3725–3740.
- [8] P. Nithiarasu, T. Sundararajan, K.N. Seetharamu, Double-diffusive natural convection in a fluid saturated porous cavity with a freely convecting wall, International Communications in Heat and Mass Transfer 24 (8) (1997) 1121–1130.
- [9] R. Bennacer, A. Tobbal, H. Beji, P. Vasseur, Double diffusive convection in a vertical enclosure filled with anisotropic porous media, International Journal of Thermal Sciences 40 (1) (2001) 30–41.
- [10] R. Bennacer, H. Beji, A.A. Mohamad, Double diffusive convection in a vertical enclosure inserted with two saturated porous layers confining a fluid layer, International Journal of Thermal Sciences 42 (2) (2003) 141–151.
- [11] M.J.S. de Lemos, L.A. Tofaneli, Modeling of double diffusive turbulent natural convection in porous media, International Journal Heat Mass Transfer 47 (2004) 4233–4241.
- [12] M.H.J. Pedras, M.J.S. de Lemos, Computation of turbulent flow in porous media using a low-Reynolds $k-\epsilon$ model and an infinite array of transversally displaced elliptic rods, Numerical Heat Transfer Part A–Appl. 43 (6) (2003) 585–602.

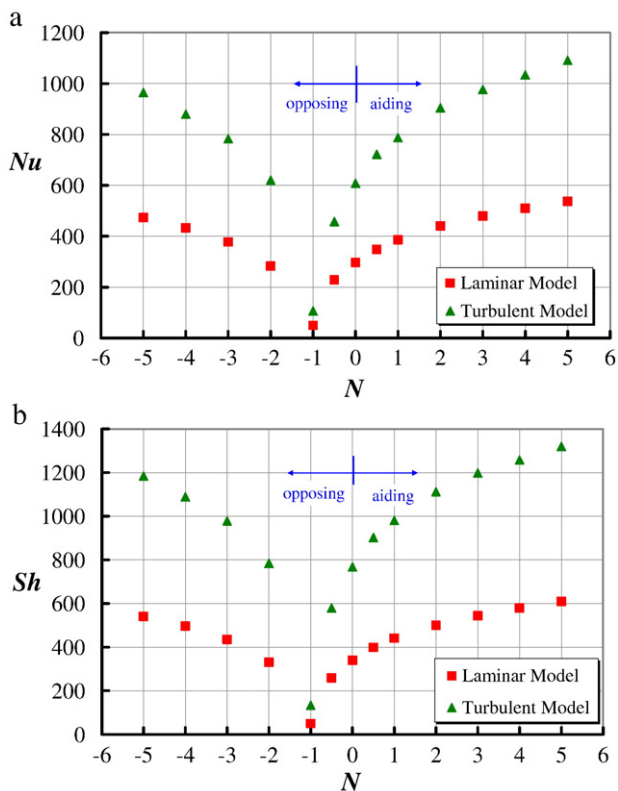


Fig. 2. Comparison of integral parameters as functions of the buoyancy ratio N for turbulent and laminar model solutions, $Ra^* = 2 \times 10^6$, $Gr_\phi = 2.25 \times 10^{10}$, $Da = 8.88 \times 10^{-6}$, $\lambda_{eff} = \lambda_s = \lambda_f$ and $\phi = 0.8$: a) Nusselt number; b) Sherwood number.

- [13] M.J.S. de Lemos, Fundamentals of the double-decomposition concept for turbulent transport in permeable media, *Materialwissenschaft und Werkstofftechnik* 36 (10) (2005) 586–593.
- [14] F.D. Rocamora Jr., M.J.S. de Lemos, Analysis of convective heat transfer for turbulent flow in saturated porous media, *International Communications Heat and Mass Transfer* 27 (6) (2000) 825–834.
- [15] E.J. Braga, M.J.S. de Lemos, Turbulent natural convection in a porous square cavity computed with a macroscopic k - ϵ model, *International Journal Heat and Mass Transfer* 47 (26) (2004) 5639–5650.
- [16] E.J. Braga, M.J.S. de Lemos, Heat transfer in enclosures having a fixed amount of solid material simulated with heterogeneous and homogeneous models, *International Journal Heat and Mass Transfer* 48 (23–24) (2005) 4748–4765.
- [17] E.J. Braga, M.J.S. de Lemos, Simulation of turbulent natural convection in a porous cylindrical annulus using a macroscopic two-equation model, *International Journal Heat and Mass Transfer* 49 (23–24) (2006) 4340–4351.
- [18] E.J. Braga, M.J.S. de Lemos, Laminar and turbulent free convection in a composite enclosure, *International Communications Heat Mass Transfer* 52 (2009) 588–596.
- [19] M.J.S. de Lemos, M.S. Mesquita, Turbulent mass transport in saturated rigid porous media, *International Communications Heat Mass Transfer* 30 (2003) 105–113.
- [20] M. Assato, M.H.J. Pedras, M.J.S. de Lemos, Numerical solution of turbulent channel flow past a backward-facing-step with a porous insert using linear and non-linear k - ϵ models, *Journal of Porous Media* 8 (1) (2005) 13–29.
- [21] N.B. Santos, M.J.S. de Lemos, Flow and heat transfer in a parallel-plate channel with porous and solid baffles, *Numerical Heat Transfer Part A–Appl.* 49 (5) (2006) 471–494.
- [22] C.T. Hsu, P. Cheng, Thermal dispersion in a porous medium, *International Journal Heat Mass Transfer* 33 (1990) 1587–1597.
- [23] J. Bear, *Dynamics of fluids in porous media*, Dover, New York, 1972.
- [24] S. Whitaker, Equations of motion in porous media, *Chem. Eng. Sci.* 21 (1966) 291.
- [25] S. Whitaker, Diffusion and dispersion in porous media, *J. Amer. Inst. Chem. Eng* 3 (13) (1967) 420.
- [26] S.V. Patankar, D.B. Spalding, A calculation procedure for heat, mass and momentum transfer in three dimensional parabolic flows, *International Journal Heat Mass Transfer* 15 (1972) 1787.
- [27] H.L. Stone, Iterative solution of implicit approximations of multidimensional partial differential equations, *SIAM J. Numer. Anal.* 5 (1968) 530–558.